Accessing quadratic nonlinearities of metals through metallodielectric photonic-band-gap structures

Giuseppe D'Aguanno,[1,*] Nadia Mattiucci,[2,1] Mark J. Bloemer,[1] and Michael Scalora[1]
[1]*Charles M. Bowden Research Center, RDECOM Building 7804, Redstone Arsenal, Alabama 35898-5000, USA*
[2]*Time Domain Corporation, Cummings Research Park, 7057 Old Madison Pike, Huntsville, Alabama 35806, USA*
(Received 29 May 2006; revised manuscript received 21 July 2006; published 11 September 2006)

We study second harmonic generation in a metallodielectric photonic-band-gap structure made of alternating layers of silver and a generic, dispersive, linear, dielectric material. We find that under ideal conditions the conversion efficiency can be more than two orders of magnitude greater than the maximum conversion efficiency achievable in a single layer of silver. We interpret this enhancement in terms of the simultaneous availability of phase matching conditions over the structure and good field penetration into the metal layers. We also give a realistic example of a nine-period, Si_3/N_4Ag stack, where the backward conversion efficiency is enhanced by a factor of 50 compared to a single layer of silver.

DOI: 10.1103/PhysRevE.74.036605 PACS number(s): 42.79.Nv, 42.65.Ky, 42.70.Qs

Metals have always been considered awkward guests for light in the realm of nonlinear optics because of their intrinsic impenetrability by the electromagnetic field across the entire spectrum. This fact notwithstanding, second harmonic generation (SHG) from the surface of metals has been one of the first nonlinear optical phenomena to be studied experimentally [1–3] and theoretically [4,5]. In Refs. [1,2] the conversion efficiencies achievable were rather small, i.e., of order 10^{-9}, because the penetration of the electromagnetic fields in a single layer of metal reduces to just a few nanometers, and the SHG process takes place in a region very close to the metal surface.

In order to get an idea about the behavior of the SHG from a single layer of metal, in Fig. 1 we show the calculated forward and backward SH conversion efficiencies at normal incidence from a single slab of silver as a function of its thickness L. The refractive index (n_{Ag}) and extinction coefficient (K_{Ag}) of silver have been taken from experimental data contained in Ref. [6]. The fundamental frequency (FF) of the pump field is $\omega_{FF}=1.269\omega_0$ with $\omega_0=2\pi c/\lambda_0$ and $\lambda_0=1\ \mu$m. The FF frequency thus corresponds to a wavelength of approximately 788 nm, and the SH field is generated at approximately 394 nm. At the FF and SH frequencies the refractive indices and extinction coefficients of silver are, respectively [6], $n_{Ag,FF}\cong 0.14$, $n_{Ag,SH}\cong 0.16$, $K_{Ag,FF}\cong 5.2$, and $K_{Ag,SH}\cong 1.9$. As regards the nonlinear quadratic coefficient of silver, here we are not concerned with its specific origin [4,5] or value, and simply suppose that $d^{(2)}_{Ag}|E_{FF,input}|=10^{-3}$, where $d^{(2)}_{Ag}$ is the quadratic nonlinear coupling coefficient of silver, and $|E_{FF,input}|$ is the strength of the input pump field. We point out that we intentionally do not give the actual value of the quadratic nonlinearity of silver, but rather we specify the value of $d^{(2)}_{Ag}|E_{FF,input}|$ on which the SH conversion efficiency depends. In fact, an analysis of the origin, or the actual value, of the quadratic coefficient of silver is outside the scope of the present work. More information about this issue can be found in Refs. [4,5,7], for example. The results presented in Fig. 1 must therefore be interpreted as a benchmark, or a reference point that may be used to estimate the SH conversion efficiency obtained from a generic structure composed of alternating layers of silver and layers of a linear, dielectric material, provided one uses and references the same product of the nonlinear coefficient and field amplitude that we use, i.e., $d^{(2)}_{Ag}|E_{FF,input}|=10^{-3}$. In doing so, the resulting enhancement factor $\eta_{structure}/\eta_{singlelayer}$ will be independent of any specific model, any input field value, and/or of the magnitude of the quadratic coefficient of silver. It is also interesting to note that the maximum conversion efficiency, which is of the order of 10^{-9} for both the forward and backward directions, is achieved in the range between 7 and 10 nm of thickness. Note also that in the limit $L\to 0$, SHG goes to zero as one may expect. Silver layers thinner than 10 nm deposited by ordinary means (thermal evaporation, sputtering, for example) may not have the same refractive index and extinction coefficient as those used here due to the fact that the bulk properties of the material may be lost. We also note that the forward and backward conversion efficiencies have simi-

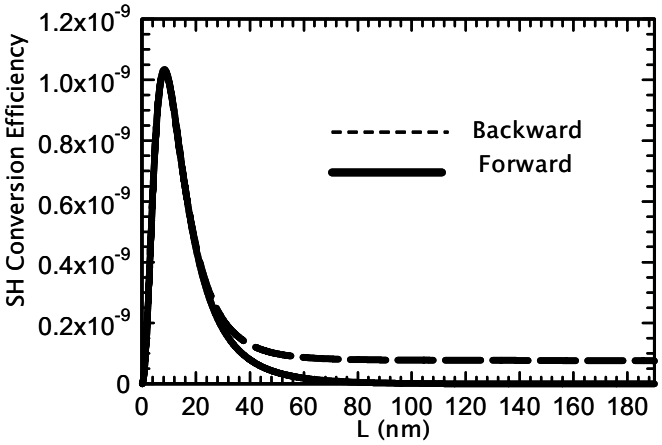

FIG. 1. Forward and backward second harmonic conversion efficiencies from a single layer of silver vs its thickness L.

*Corresponding author. FAX: 001-256-8422507.
Electronic address: giuseppe.daguanno@us.army.mil or giuseppe.daguanno@gmail.com

lar magnitudes for silver layers whose thickness does not exceed 25 nm. For thicker layers, the forward conversion efficiency decreases dramatically, while the backward conversion efficiency tends to a saturation value of the order of 7×10^{-11}. Therefore in what follows we will consider 10-nm-thick silver layers.

Although the first thin film metallodielectric interference filters date back to 1939 [8], some important aspects of light propagation in such structures had not been investigated until recently, when it was demonstrated [9,10] that the stratification of metals and dielectric materials in the form of a metallodielectric photonic-band-gap structure (MDPBG) could create transparency regions in the visible range and well into the Drude region. The work done in Refs. [9,10] has thus highlighted the use of metals in devices that require high transparency, MDPBGs in particular, and the possibility to use MDPBGs to access, for example, the high cubic nonlinearities of metals, Cu in particular [11]. The first theoretical study on the possibility to access the cubic nonlinearity of Cu using MDPBGs can be found in Ref. [11], and a subsequent experimental verification in Ref. [12]. Using a similar mechanism, MDPBGs that contain Cu metal have also been theoretically predicted to function as broadband optical limiting devices that operate across the entire electromagnetic spectrum [13].

In this paper we show that MDPBGs can also be used to access the quadratic nonlinearity of metals. The issue of accessing quadratic nonlinearities of metals is much more delicate than the issue of accessing their cubic nonlinearities. In fact, while in the case of cubic nonlinearities the only crucial condition is the achievement of good penetration of the electric field into the metal layers, in the case of quadratic nonlinearities good field penetration should also be accompanied by coherent oscillations of the nonlinear dipoles, i.e., phase matching conditions. In Fig. 2 we show the linear transmission at normal incidence of a $N=10$-period MDPBG made of alternating layers of silver and a generic, linear dielectric material (D). The thicknesses of dielectric material and silver layers are, respectively, $a=100$ nm (D) and $b=10$ nm (Ag), and the structure has a total length of $L=1.1$ μm. The arrows in the figure indicate the tuning conditions of the FF and SH fields. We will have more to say about these particular tuning conditions later, when we discuss the structure in more detail.

We now describe the properties of the dielectric material. The electric susceptibility of the dielectric material is described through a Lorentz model: $\epsilon_D(\tilde{\omega})=\epsilon_\infty-A_D/(\tilde{\omega}^2-\omega_{0R}^2+i\gamma_D\tilde{\omega})$, where $\epsilon_\infty=(4.06)^2$, $A_D=1$, $\omega_{0R}=1.3695$, $\gamma_D=6.25\times10^{-4}$, and $\tilde{\omega}=\omega/\omega_0$ is the normalized frequency. The refractive indices (n) and the extinction coefficients (K) of the dielectric material at the FF and SH frequency are, respectively, $n_{D,FF}\cong4.5$, $K_{D,FF}\cong1.3\times10^{-3}$, $n_{D,SH}\cong4.03$, $K_{D,SH}\cong9.4\times10^{-5}$. These values of refractive index and extinction coefficient do not refer to any dielectric or semiconductor material in particular. In fact, for the time being, we seek to establish proof of principle of the effect and, perhaps more importantly, to discuss the physical mechanisms that lay behind the effect. Later we will discuss the possibility to use ordinary dielectric materials such as ITO, Si_3N_4, TiO_2, for example. In Figs. 3 we show the FF pump field and the SH generated field inside the structure for $d_{Ag}^{(2)}|E_{FF,input}|=10^{-3}$. The calculations have been carried out using a rigorous Green function approach as detailed in Refs. [14,15]. Several considerations are in order.

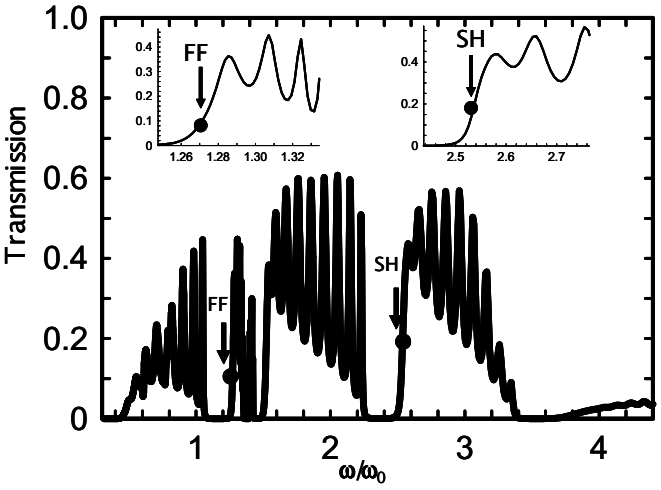

FIG. 2. Transmission (T) at normal incidence vs ω/ω_0 for a structure made of $N=10$ periods of alternating layers of dielectric material and silver. The thicknesses of the dielectric material and of the silver are, respectively, $a=100$ nm and $b=10$ nm. The structure is surrounded by air. The arrows and the full circles indicate the tuning of the FF and SH field. Inset: magnification of the tuning conditions.

First, from Fig. 3(b) one realizes that the backward conversion efficiency is approximately 1.45×10^{-7}, and the forward conversion efficiency is approximately 5.42×10^{-8}. These conversion efficiencies compare rather well with the conversion efficiency from a single, 10-nm layer of silver, with enhancement factors of 145 for the backward direction, and 54 for the forward direction. In sum, we obtain a total conversion efficiency more than two orders of magnitude

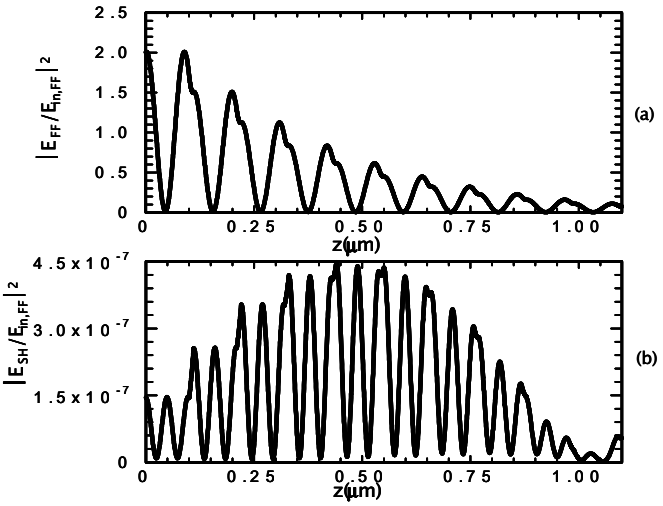

FIG. 3. Field localization over the structure for the FF pump field [Fig. 3(a)] and for the SH generated field [Fig. 3(b)]. We suppose that $d_{Ag}^{(2)}|E_{FF,input}|=10^{-3}$ as in the case of the single slab of silver.

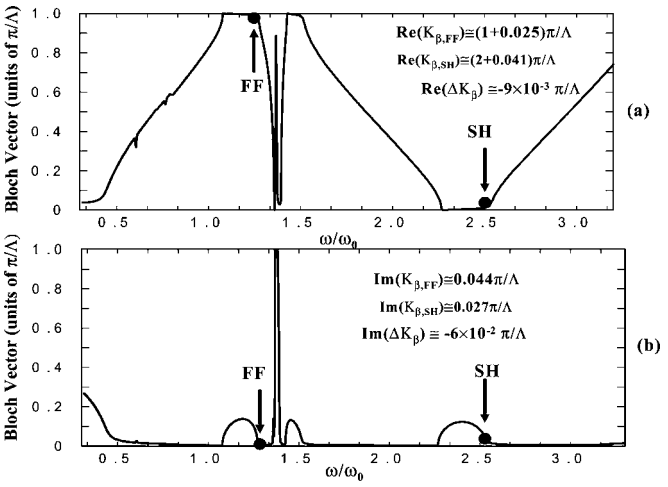

FIG. 4. (a) Real part of the Bloch vector vs ω/ω_0. (b) Imaginary part of the Bloch vector vs ω/ω_0. $\Lambda=a+b$ is the length of the elementary cell. $\Delta K_\beta=K_\beta(2\omega)-2K_\beta(\omega)$ is the wave-vector mismatch. Note that for our tuning conditions a quasiperfect phase matching is achieved.

greater than the maximum SHG achievable in a single layer of silver. Second, from Fig. 3(a) we note that the FF field is able to penetrate quite well inside each metal layer. In particular, the electric field intensity inside the first two layers of metal is even greater than its value at the input.

As we mentioned earlier, field localization inside the metal is just one of the two key concepts that allow an efficient process to take place. The second required ingredient is the availability of phase matching conditions. In Fig. 4 we show the Bloch vector (K_β) for the ten-period structure. The figure shows that perfect phase matching conditions are nearly achieved: we have $\mathrm{Re}(\Delta K_\beta)\cong -9\times 10^{-3}\pi/\Lambda$ and $\mathrm{Im}(\Delta K_\beta)\cong -6\times 10^{-2}\pi/\Lambda$, where $\Delta K_\beta=K_\beta(2\omega)-2K_\beta(\omega)$ is the Bloch wave-vector mismatch. In Fig. 5 we show the second harmonic conversion efficiency as a function of the number of periods for the same elementary cell used in the ten-period structure. The FF and SH fields remain tuned to the same frequency, i.e., $\omega_{\mathrm{FF}}=1.269\omega_0$ and $\omega_{\mathrm{SH}}=2.538\omega_0$.

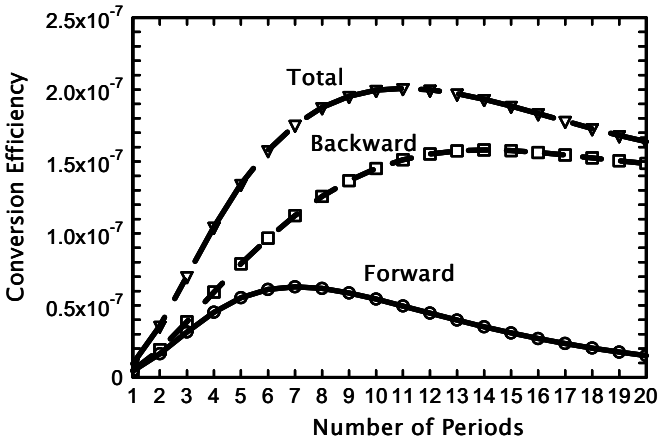

FIG. 5. SH conversion efficiency vs the number of periods (N).

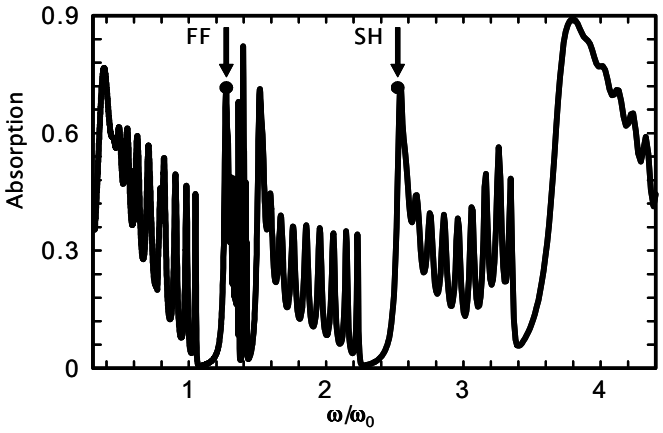

FIG. 6. Absorption at normal incidence ($A=1-R-T$) vs ω/ω_0. The arrows indicate the tuning of the FF and SH fields.

The optimal structure will depend on the particular application one is seeking. For example, the maximum conversion efficiency in the forward direction is achieved for $N=7$ periods, the maximum backward conversion efficiency is achieved for $N=14$ periods, and the maximum total conversion efficiency is achieved for $N=11$ periods.

In order to be as clear as possible regarding the physical mechanism behind the enhancement of the SHG and, more importantly, in order to give a general recipe on how to find the "ideal conditions" that we have described so far, let us show in Fig. 6 the absorption ($A=1-R-T$) for the ten-period MDPBG. The figure shows that the FF and SH happen to be tuned at the two peaks of absorption of the structure, respectively, near the first and near the second band gap. Those peaks of absorption do not correspond to peaks of transmission, as one may easily ascertain by looking at the tuning conditions on the transmission function showed in Fig. 2. Although at a first sight this result may appear as a counterintuitive result, as a matter of fact it is not counterintuitive. In fact, taking into account that the extinction coefficient of the dielectric material at both the FF and the SH frequency is quite low ($K_{\mathrm{D,FF}}\cong 1.3\times 10^{-3}$, $K_{\mathrm{D,SH}}\cong 9.4\times 10^{-5}$), the high absorption is an indication that the electromagnetic field is penetrating quite well into the metal layers.

Of course, this is valid in the spectral regions where the absorption of the dielectric material can be considered negligible. For example, in Fig. 6, the absorption resonances near $1.4\omega/\omega_0$ are due to the resonance line of the Lorentz model for the dielectric material and therefore, of course, they are not an indication that the field is penetrating well into the metal layers. Put another way, if the absorption of the dielectric material can be considered negligible, then the absorption function $A(\omega)$ in a MDPBG plays, in some sense, a role analogous to the role played by the transmission function $T(\omega)$ in conventional all-dielectric PBGs. Now, in the structure which we have described, not only both the FF and SH fields have the best possible penetration inside the metal layers, but also the structure is designed so that the perfect phase matching condition is achieved for those frequencies. Of course, we are not saying that in every MDPBG made with real materials the two conditions will be always simul-

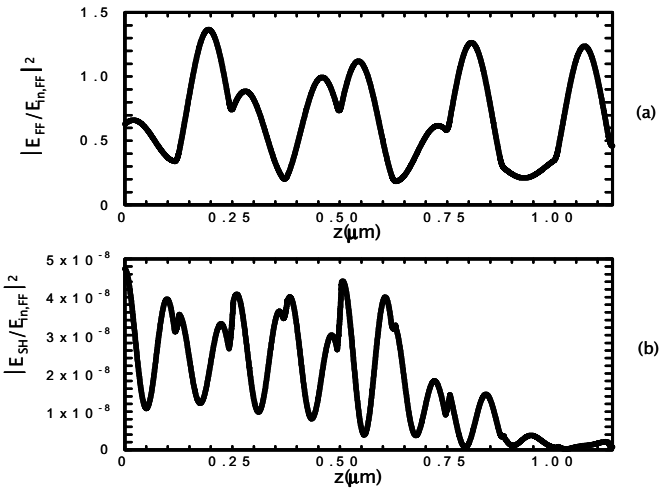

FIG. 7. Field localization over the structure for the FF pump field [Fig. 6(a)] and for the SH generated field [Fig. 6(b)]. We suppose that $d_{\mathrm{Ag}}^{(2)}|E_{FF,input}|=10^{-3}$ as in the case of the single slab of silver. The structure is made of $N=9$ periods, composed of alternating layers of Si_3N_4/Ag. The thickness of the layers is, respectively, $a=116$ nm (Si_3N_4) and $b=10$ nm (Ag). The FF field is tuned at 795 nm.

taneously available. Here we have just showed the general recipe that should be followed in order to achieve high conversion efficiencies from a MDPBG structure, supposed that the only available source of quadratic nonlinearity is that of the metal layers.

Now that we have discussed the physical mechanisms behind the possibility to access quadratic nonlinearities of metals, let us go back to the issue of using ordinary dielectric materials, such as ITO, Si_3N_4, TiO_2, for example. In Fig. 7 we show the FF field intensity profile, and the generated SH field intensity normalized with respect to the incident FF intensity value, in a $N=9$-period structure composed of alternating layers of Si_3N_4 and Ag. As is well known, Si_3N_4 has a refractive index $n\cong 2$ across the visible and near infrared (IR) ranges [6]. The FF field is tuned at $\omega_{\mathrm{FF}}=1.258\omega_0$, which corresponds to a wavelength of 795 nm. The thickness of each of the Si_3N_4 layers is 116 nm, while Ag layers are each 10 nm thick. The figure suggests that we obtain a SH backward conversion efficiency of 4.74×10^{-8}, i.e., approximately 50 times greater than the maximum backward conversion efficiency achievable in a single layer of Ag. A Bloch vector analysis reveals that the structure has a moderately small phase mismatch, i.e., $\mathrm{Re}(\Delta K_\beta)\cong 0.26\pi/\Lambda$. In this case, the SH signal is almost totally generated in the backward direction. We point out that in this case only the SH is tuned at the highest peak of absorption and also we point out that the phase matching is not perfect, those two factors are basically responsible for the decreasing of the enhancement factor with respect to the ideal structure that we have described before. By the way, this example should make it clear that the kind of structure we are envisioning, which effectively combines field penetration and phase matching conditions in metals in an unprecedented manner, could be easily fabricated using standard sputtering or thermal evaporation techniques [8,10]. We observe that the example we have provided by no means exhausts the possible variations on structure design that could be implemented to preserve the two mechanisms that together conspire to dramatically improve conversion efficiency: good field penetration and relatively favorable phase matching conditions. Finally, we add that the results we have presented have been completely validated in the short pulse, subpicosecond regime. The simulation code used in the short pulse regime has also been successfully applied to the study of broadband optical limiting in MDPBGs and more details about it can be found in Ref. [13].

In conclusion, we have shown that MDPBGs may hold the key to access the quadratic nonlinearities of metals, thanks to the simultaneous availability of phase matching conditions and good penetration of the field into the metal layers. We expect that the type of devices we have proposed will have important applications for SHG and nonlinear frequency conversion in general, and it is hoped that our results will stimulate new research directed at developing these unique structures.

Giuseppe D'Aguanno thanks the NRC for financial support.

[1] F. Brown, R. E. Parks, and A. M. Sleeper, Phys. Rev. Lett. **14**, 1029 (1965).
[2] N. Bloembergen *et al.*, Phys. Rev. **174**, 813 (1968).
[3] Y. R. Shen, *The Principles of Nonlinear Optics* (Wiley, New York, 1984).
[4] S. S. Jha, Phys. Rev. Lett. **15**, 412 (1965).
[5] H. Cheng and P. B. Miller, Phys. Rev. **134**, A683 (1964).
[6] *Handbook of Optical Constants of Solids*, edited by E. D. Palik (Academic, New York, 1985).
[7] D. Krause, C. W. Teplin, and C. T. Rogers, J. Appl. Phys. **96**, 3626 (2004).
[8] H. A. Macleod, *Thin-Film Optical Filters* (Institute of Physics Publishing, 2001).
[9] M. Scalora *et al.*, J. Appl. Phys. **83**, 2377 (1998).
[10] M. J. Bloemer and M. Scalora, Appl. Phys. Lett. **72**, 1676 (1998).
[11] R. S. Bennink, Y. K. Yoon, R. W. Boyd, and J. E. Sipe, Opt. Lett. **24**, 1416 (1999).
[12] N. N. Lepeshkin, A. Schweinsberg, G. Piredda, R. S. Bennink, and R. W. Boyd, Phys. Rev. Lett. **93**, 123902 (2004).
[13] M. Scalora *et al.*, Phys. Rev. E **73**, 016603 (2006).
[14] G. D'Aguanno, N. Mattiucci, M. Scalora, M. J. Bloemer, and A. M. Zheltikov, Phys. Rev. E **70**, 016612 (2004).
[15] N. Mattiucci, G. D'Aguanno, M. J. Bloemer, and M. Scalora, Phys. Rev. E **72**, 066612 (2005).